

PAPER • OPEN ACCESS

Microfabrication of Alkali Vapor MEMS Cells for chip-scale atomic clock

To cite this article: A Kazakin *et al* 2021 *J. Phys.: Conf. Ser.* **2103** 012188

View the [article online](#) for updates and enhancements.

You may also like

- [The influence of protein levels on body weight, body dimensions, and reproductive characteristics of local chickens treated in-ovo feeding L-Arginine for two generations](#)
W Pakiding, M R Hakim, Daryatmo et al.
- [Evaluations of successful practices in the implementation of green management](#)
R M Lamzin, D A Mosolova and O A Knyazhechenko
- [Location Problem of Production and Sales under Carbon Tax Policy](#)
Chong Xiang, Xiaoshen Li and Guanglei Sun

Microfabrication of Alkali Vapor MEMS Cells for chip-scale atomic clock

A Kazakin¹, R Kleimanov¹, I Komarevtsev¹, A Kondrateva¹, Y Enns¹,
A Shashkin² and A Glukhovskoy³

¹ Peter the Great St Petersburg Polytechnic University, 195251 St Petersburg, Russia

² S.I. Vavilov State Optical Institute, 192171 St Petersburg, Russia

³ IMPT, Gottfried Wilhelm Leibniz Universität Hannover, 30823 Garbsen, Germany

e-mail: kazakin75@gmail.com

Abstract. The technology of MEMS atomic cells containing rubidium or caesium vapors in an atmosphere of neon buffer gas has been developed. Two-chamber silicon cells containing an optical cavity, shallow filtration channels and a technical container for a solid-state alkali source have been implemented in a single-step process of anisotropic wet chemical etching. To prevent significant undercutting of the filtration channels during etching of the through silicon cavities, the shapes of the compensating elements at the convex corners of the silicon nitride mask have been calculated and the composition of the silicon etchant has been experimentally found. The sealing of the cells has been carried out by silicon-glass anodic bonding at a temperature of 250 °C. For this purpose the LK5 glass which has an increased ionic conductivity in comparison with the conventional glass Borofloat 33 was used. The best microfabricated cells allowed us to obtain estimates of the relative instability of the coherent population trapping resonance frequency at the level of $5 \cdot 10^{-11}$ at 1 s.

1. Introduction

Miniature gas cells containing alkali metal vapors are key elements of quantum magnetometers, atomic clocks, and other quantum devices [1], that are used in atomic spectroscopy [2], medical diagnostics [3], telecommunications, and navigation systems [4]. Development of technologies of microelectromechanical systems (MEMS) and vertical-cavity surface-emitting lasers (VCSEL) made it possible to create miniature chip-scale atomic clocks (CSAC) based on the coherent population trapping (CPT) effect [5–7].

Unlike the first MEMS cells with a single absorption chamber [5], modern cells for CSAC have a two-chamber design [8]. They consist of two etched in silicon cavities with a volume of several cubic millimeters connected by narrow filtration channels. At the bottom and top sides, the cavities and channels are hermetically sealed with transparent borosilicate glasses that are thermomechanically compatible with silicon (Pyrex 7740, Borofloat 33, Hoya SD-2, etc). One of the cavities is used to fill the cell with a solid-state alkali dispenser, which contains a reducing agent and an alkali metal salt. The other cavity contains only pure alkali metal vapors and an inert buffer gas (He, N₂, Ne, Ar, etc) and provides optical absorption at a wavelength corresponding to the atomic line D1 of ¹³³Cs, ⁸⁵Rb or ⁸⁷Rb isotopes. Filtration channels provides, due to a small cross-section, a transfer of alkali vapors from dispenser cavity into the optical cavity without byproducts and contaminations formed during



laser activation of the solid-state source [9]. The main processes of the MEMS cells technology are through-wafer etching of silicon, filling with an alkali metal source and vacuum-tight sealing of the cell in the appropriate buffer atmosphere.

Deep anisotropic alkaline etching of silicon is excellent for making of single-chamber cells [5]. However, it is difficult to form compact two-chamber cells with an optical path length of about 1 mm by alkaline etching due to excessive undercutting of the filtration channels at the convex corners of the mask. For this reason, the cells of the described design are mainly made by plasma-chemical etching of silicon. In addition to the high cost, plasma-chemical etching is accompanied by a high roughness of the optical cavity walls and the polymer contaminants formation [8]. This leads to the need for additional smoothing of the walls by wet etching, which further increases the cost of the technology.

The choice of the method and technological conditions of cell sealing is limited by the temperature of thermal destruction of the used source of alkali metal vapors [9]. The most suitable method for industrial cell manufacturing is the anodic bonding of silicon with Pyrex 7740 and Borofloat 33 glasses. Anodic bonding ensures sufficient quality of cell sealing at temperatures above 300 °C [11]. For this reason, this method is poorly suited for the manufacture of cells with sources of alkali metal vapors based on their azides and chlorides with lower decomposition temperatures [1], as well as cells with anti-relaxation wall coatings based on organosilanes [12]. Reducing the cells sealing temperature can be achieved by using new materials for the anode bonding with silicon.

This work is dedicated to the development and implementation of a mass production technology of MEMS cells for CSAC containing vapors of ^{87}Rb or ^{133}Ce isotopes in neon atmosphere. The two-chamber cells have been fabricated in a single-step alkaline etching of silicon, followed by sealing with LK5 glass by anodic bonding at low temperatures.

2. MEMS atomic vapour cells microfabrication

2.1. Process flow of fabrication

The cells were made in the form of chips with a total size of 6 x 6 x 1.6 mm. Their basic design contained two volumetric cavities with sizes of 3 x 1.5 x 0.6 mm, connected by rectangular channels with a length of 1 mm and a width of 100 – 200 μm (figure 1). Depending on the manufacturing conditions, the real appearance of the chips could differ from the basic design (figure 2).

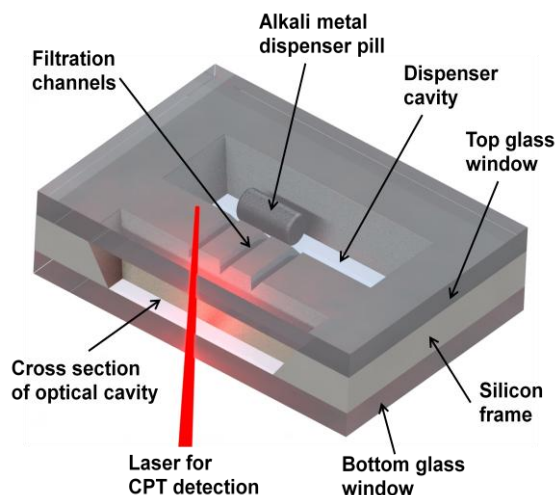


Figure 1. Two-chamber cell scheme.

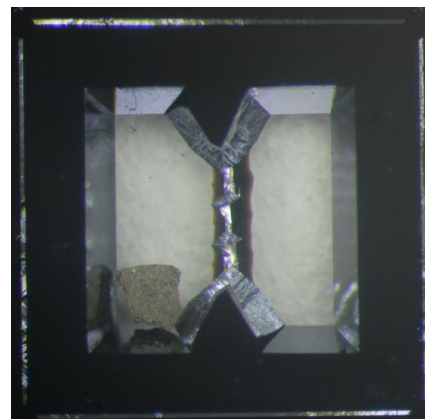


Figure 2. The MEMS cell with ^{87}Rb vapor, made by the authors in 2014.

The process of alkali vapor cells fabrication is shown in figure 3. A (100)-oriented n-type silicon wafer of 3" (KEF-7.5 with a thickness of 400 or 600 μm) and two borosilicate glass wafer

(Borofloat 33 or LK5 glasses with a thickness of 450 μm) are used for cells fabricate. The both surfaces of the wafers are polished prior to the process. First, a mask layer of silicon nitride with a thickness of 200 nm is deposited on both sides of the silicon wafers. An array of the optical and dispenser cavities (through-wafer holes) and the filtration channels (V-grooves trenches with a depth of 280 μm) are patterned on Si wafer by photolithography and etched in a Si wafer by anisotropic wet etching in potassium hydroxide (KOH) solution (figure 3a).

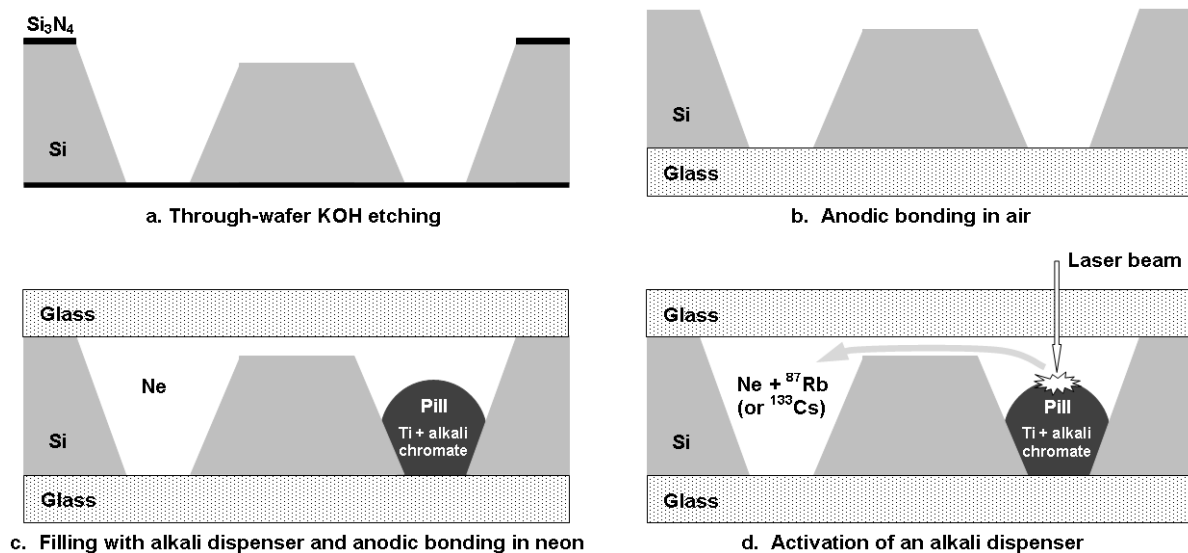


Figure 3. Cell fabrication process.

At the second stage, the nitride layer is removed, followed by anodic bonding of the silicon wafer with the bottom glass. Bonding is carried out in air at 400 $^{\circ}\text{C}$ and 800 V for 30 minutes (figure 3b). Subsequently, Cs- or Rb-containing microsources are inserted in the dispenser cavities of every cell. As a source of alkali metal vapors, micropills made by sintering titanium powders with 7% rubidium or caesium bichromate are used.

The vacuum-tight sealing of the cells is carried out in a laboratory anodic bonding system, equipped with a gas line for the supply of inert gases (figure 3c). Neon is used as a buffer gas at a pressure of 100 to 400 Torr. The specific value of the neon pressure in the cells for CSAC is selected on the basis of previous experimental work [13]. At the final stage (figure 3d), the plates are divided into separate chips, followed by the activation of the micropills by laser heating according to a well-known technique [8].

2.2. Optimization of the mask topology for single-step alkaline etching of two-chambers cell

The formation of the internal volume of the cell by alkaline etching can be carried out in two stages to separately form through-wafer cavities and V-grooves filtration channels. However, this way requires performing of several photolithography operations, processes for removing and deposition of masking coatings, precise alignment of topologies with photomasks, or photolithography on the surface with deep relief. To reduce the cost of cells technology, a single-step alkaline etching for the simultaneous formation of cavities and channels has been developed. An obstacle to this process is the excessive undercutting of the filtration channels at the convex corners of the mask, i.e. in places where the channels connect to the cavities. This is due to the increased rate of dissolution of silicon facets with high Miller indexes ($\{311\}$, $\{411\}$ and etc) with respect to the direction $\langle 100 \rangle$. More information about the reasons of convex corners undercutting can be found in the review [10]. As a result, during the deep Si etching ($> 400 \mu\text{m}$) at normal conditions (30% aqueous solution of KOH at 80 $^{\circ}\text{C}$), the cell filtration channels with a length of 1 mm disappear and optical and dispenser cavities completely

transform into one large cavity, as can be seen in figure 2. The use of longer channels in the cell design would lead to an increase in the size of the chip. But it is possible to compensate for the undercutting of convex corners by a suitable mask design. For this purpose, compensation elements of various geometries at all convex corners of the mask are used – triangle, square, $\langle 110 \rangle$ -oriented beam, $\langle 100 \rangle$ -oriented beam, superimposed squares and etc.

Using the formulas from [10], we performed a preliminary analytical calculation of the shape and size of these compensation elements, which are suitable for the design of our cell geometry. Also, the program ACES has been used to simulate the process of etching silicon to a depth of 600 microns in alkaline etchants with different compositions and concentrations. Data on the etching rates of different silicon facets were taken from [14]. Due to the limited space for their placement in the cavities, two variants of convex corners undercutting compensators were chosen – square with a side W of 700 μm and $\langle 110 \rangle$ -oriented beam with a length L of 1 mm. The design of the nitride mask with these elements is shown in the insertions at the upper-left corner in figure 4a and figure 4b.

To reduce the rate of filtration channels undercutting, aqueous KOH solutions with additives of isopropyl alcohol (IPA) have been used. It is known that alcohol additives in KOH etchants reduce the rate of dissolution of the $\{311\}$ silicon facet [14]. The best results for the cells fabrication have been obtained with an etchant consisting of equal volumes of 30% KOH and IPA. Silicon etching has been carried out at a temperature of 80 $^{\circ}\text{C}$ in a container with a cooled lid to prevent the alcohol evaporation. After 8 hours of etching, the cell cavities have been etched through and the undercutting compensators have been completely dissolved, leaving the V-groove filtration channels open. Figure 4 shows the photos of the cells formed by this method (after the final stages of the cells process flow).

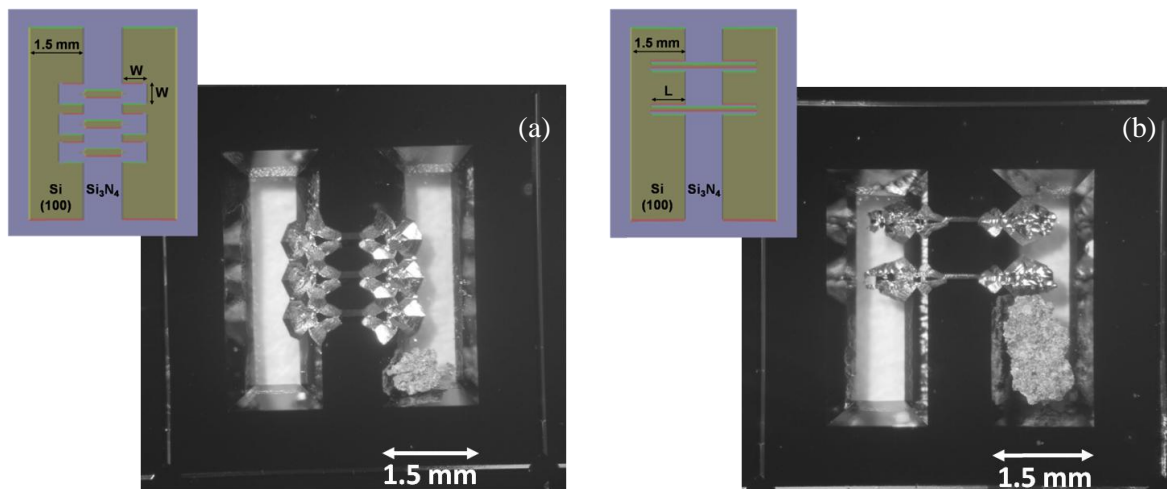


Figure 4. Cells made by alkaline etching in KOH : IPA solution with the mask with compensators of the square type (a) and $\langle 110 \rangle$ -oriented beam type (b).

2.3. Selection of glass for anodic sealing of cells

To implement the procedure of cells anodic sealing, a comparative study of Borofloat 33 glass and its domestic analogue, LK5 glass, has been carried out.

Both glasses have approximately the same coefficients of thermal expansion, close to single-crystal silicon [15], but their compositions are slightly different [16]. For this reason, the optical transmittance of glass wafers with a thickness of 450 μm has been measured. The spectral dependences shown in figure 5 prove an almost complete identity of the transmittance of both glasses at the wavelengths 794.8 nm and 894.6 nm, corresponding to the atomic line D1 of ^{87}Rb and ^{133}Cs isotopes, respectively.

The measurement of the temperature dependences of the electrical conductivity of the Borofloat 33 and LK5 glasses has been carried out. Prior to the measurement, each glass wafer has been cleaned in piranha solution and rinsed in deionized water, followed by sputtering of aluminum blocking

electrodes on both sides of wafer. For the glass conductivity measurement, equipment designed for anodic bonding of silicon and glass has been used. The conductivity of each glass at a given temperature was estimated by the value of the initial current jump at the moment of switching on the voltage. The measured dependencies are shown in Figure 6.

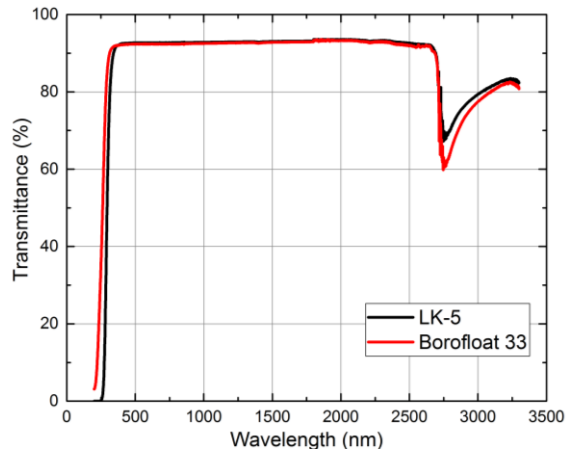


Figure 5. Optical transmittance of Borofloat 33 and LK5 glasses.

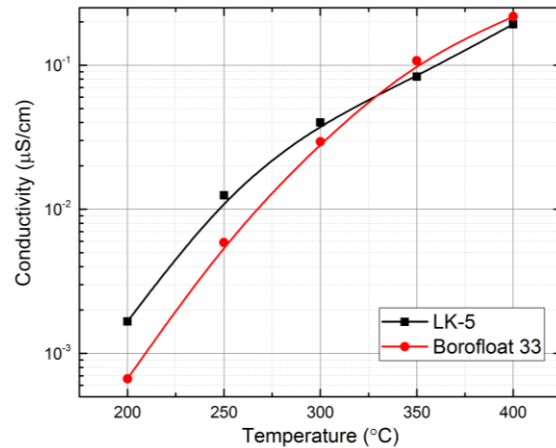


Figure 6. Electrical conductivity of Borofloat 33 and LK5 glasses.

At standard temperatures for the anodic bonding ($> 350\text{ }^{\circ}\text{C}$), the conductivities of both glasses are approximately equal. However, in the temperature range of $200 - 300\text{ }^{\circ}\text{C}$, the ionic conductivity of LK5 glass exceeds the conductivity of Borofloat 33 glass by about two times. This fact is important for the sealing of cells in the neon atmosphere at pressures of several hundred Torr, because it allows us to achieve a hermetic silicon-LK5 bonding at lower temperatures and volts.

Anodic sealing at low pressures of noble gases differs from sealing in a standard air atmosphere due to the occurrence of a gas breakdown in the bonding chamber at voltages lower than necessary for a high-quality bonding. Figure 7b shows the measured values of the breakdown voltage in our bonding chamber as a function of the neon pressure. In the case of Borofloat 33 glass, this fact leads to the need to use a complex two-stage process of anodic sealing – prebonding in neon at low volts and subsequent bonding in air at high volts [8].

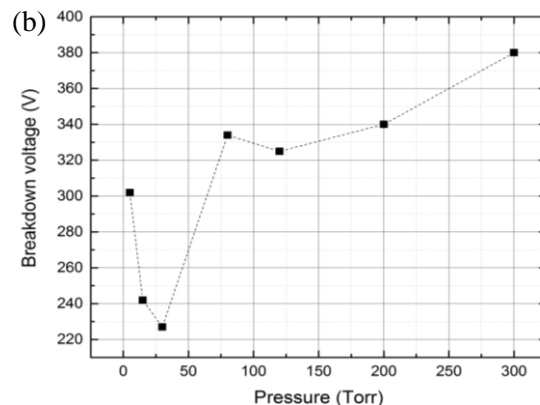
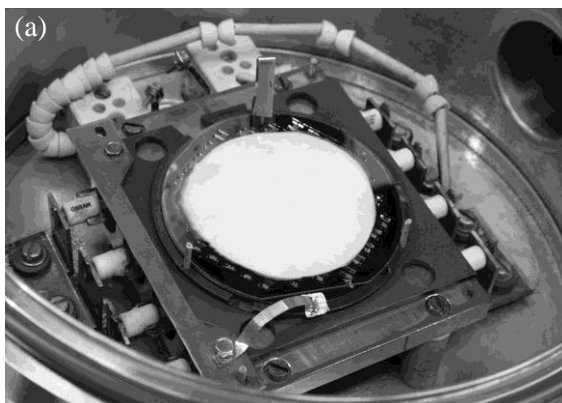


Figure 7. Sealed 3" glass-silicon-glass wafer with the atomic cells in bonding chamber (a) and breakdown voltage in bonding chamber as a function of the neon pressure (b).

The use of LK5 glass, which has increased electrical conductivity in comparison with the classic MEMS glasses, made it possible to perform vacuum-tight anodic sealing of the cells at voltages of

320 – 360 V, depending on the neon pressure, and low bonding temperatures, about 250 °C. Anodic bonding has been carried out in a tool that provides a gap between the wafers for vacuuming and degassing the cells cavities (figure 7a). Previously, a thin-film aluminum cathode has been sputtered on the reverse side of the top glass wafer. The sequence of operations for cells encapsulation with LK5 glass was as follows: annealing and degassing the wafers with a gap between them in vacuum (350 °C, 0.5 mTorr, 1 hour), cooling to room temperature, introduction of neon, annealing to 250 °C, applying the contact force on wafers, anodic bonding for 2 hours, cooling. After sealing, the aluminum cathode coating with the sodium released on the outside of the top glass has been removed by wet etching (the glass wafer remained transparent). Then the glass-silicon-glass wafer with the gas cells has been divided into chips and the laser activation of the alkali dispenser has been carried out.

3. Results

The operability of the fabricated cells has been confirmed by studies on the measurement of the CPT-signal according to the methods described in the works [6, 7, 13]. Studies of manufactured cells from various series, containing ^{133}Cs and ^{87}Rb atoms at different pressures of the neon buffer gas (200 – 400 Torr), for the width and intensity of the Hanle and CPT signals showed acceptable reproducibility of the cell parameters (the dispersion of parameters from 30% to 50%). This dispersion can be explained by differences in the modes of laser activation of cells. The best cell samples allowed us to obtain estimates of the relative instability of the CPT-resonance frequency at the level of $5 \cdot 10^{-11}$ at 1 s.

The developed technology has advantages for chip-scale atomic clock mass production. For the fabrication of two-chamber alkali vapor cells, only one photolithography and a cheap process of alkaline silicon etching are used. The sealing of the cells is carried out by the anodic bonding of silicon and LK5 glass at a relatively low temperature of 250 °C.

Acknowledgments

This work was carried out in Peter the Great St.Petersburg Polytechnic University and was supported by a grant of Russian Science Foundation (project № 20-19-00146).

References

- [1] Kitching J 2018 *Appl. Phys. Rev.* **5** 031302
- [2] Knapkiewicz P 2018 *Micromachines* **9** 405
- [3] Bobrov M A et al 2020 *J. Phys.: Conf. Ser.* **1697** 012175
- [4] Lozov R K et al 2019 *J. Phys.: Conf. Ser.* **1236** 012077
- [5] Knappe S 2008 *Compr. Microsyst.* **3** 571–612
- [6] Ermak S V et al 2015 *St. Petersburg Polytech. Univ. J. Phys. Math.* **1** 37–41
- [7] Bobrov M A et al 2019 *J. Phys.: Conf. Ser.* **1400** 077014
- [8] Hasegawa M et al 2011 *Sens. Act. A* **167** 594–601
- [9] Knapkiewicz P 2019 *Micromachines* **10** 25
- [10] Pal P and Sato K 2015 *Micro and Nano Syst. Lett.* **3** 6
- [11] Dziuban J A 2006 *Bonding in Microsystem Technology (Springer Series in Advanced Microelectronics vol 24)* ed K Itoh et al (Netherlands: Springer) pp 204-9
- [12] Ji Y et al 2017 *IEEE 67th Electronic Components and Technology Conference (ECTC)*, Orlando, FL, USA, 2116-20
- [13] Fedorov M I et al 2016 *J. Phys.: Conf. Ser.* **769** 012046
- [14] Zubel I et al 2001 *Sens. Act. A* **87** 163–71
- [15] Sinev L S and Ryabov V T 2017 *J. Micro/Nanolith. MEMS MOEMS* **16**(1) 015003
- [16] Sinev L S 2018 Calculation and selection of silicon to glass anodic bonding modes based on the criterion of minimum residual stress *Preprint arXiv:1804.08644 [physics.app-ph]* p 39